Hypersonic acoustic-phonon emission from two-dimensional electron gases in the presence of spin-orbit interaction

W. Xu*

Department of Theoretical Physics, Research School of Physical Sciences and Engineering, Australian National University, Canberra, ACT 0200, Australia

(Received 14 March 2003; revised manuscript received 22 August 2003; published 24 November 2003)

The unique feature of electron interaction with acoustic-phonons is studied theoretically for a two-dimensional electron gas (2DEG) in the presence of spin-orbit (SO) interaction (SOI) induced by the Rashba effect. The presence of SOI in a 2DEG can open up new channels for electronic transitions. As a result, acoustic-phonon emission can be generated via intra- and inter-SO electronic transitions around the Fermi level. However, it is found that due to selection rules induced by momentum and energy conservation during an electron–acoustic-phonon scattering event, the intensity of the acoustic-phonon generation can be slightly reduced by SOI. The frequency and angular dependence of the acoustic-phonon emission on SOI in an InGaAs-based 2DEG has been examined.

DOI: 10.1103/PhysRevB.68.205329 PACS number(s): 63.20.Kr, 71.70.Ej

I. INTRODUCTION

Phonon oscillations in semiconductors can provide high-frequency hypersonic sources with terahertz (10^{12} Hz or THz) sound frequency for optic-phonons and sub-THz frequency for acoustic-phonons. Phonon generation and scattering by nonequilibrium electrons in two-dimensional electron gas (2DEG) systems have been of considerable interest due to their paramount importance in semiconductor physics and in device applications.[1] In semiconductor-based 2DEG systems, phonon scattering affects significantly the physical properties and emission and absorption of phonons by electrons can lead to the realization of acoustic devices such as high-frequency hypersonic generators.[2] It has been realized that hypersonic acoustic-phonon emission from semiconductor-based 2DEGs can be generated either optically[3] or electrically[1,4] through electronic transition around the Fermi level. Over the past two decades or so, acoustic-phonon generation from *spin-degenerate* 2DEGs has been intensively investigated both experimentally[1,3–5] and theoretically.[6,7]

In recent years, significant progress has been made in realizing spin polarized electronic systems on the basis of diluted magnetic semiconductors or narrow-gap semiconductor nanostructures. One important aspect in the field of spin-electronics (or spintronics) is to investigate finite spin-splitting realized in the absence of a magnetic field *B*, because of important applications to novel electronic devices such as spin-transistors,[8] spin-waveguides,[9] quantum computers,[10] etc. It is known that in narrow-gap semiconductor quantum wells, zero-B-field spin-splitting of electrons can be achieved by the inversion asymmetry of the microscopic confining potential due to the presence of the heterojunction.[11] This inversion asymmetry corresponds to an inhomogeneous surface electric field and, hence, this kind of spin-splitting is electrically equivalent to the Rashba spin-splitting or Rashba effect.[12] The state-of-the-art material engineering and micro- or nano-fabrication techniques have made it possible to achieve experimentally observable Rashba effect in, e.g., InAs- and InGaAs-based 2DEG systems.[13–15] At present, most of the published work is focused on the effect of spin-orbit interaction (SOI) on electronic and transport properties of the spintronic devices. In order to explore the new applications of the spintronic systems as acoustic devices such as high-frequency hypersonic sources, it is important and necessary to examine the features of electron-phonon scattering in a spin split 2DEG. Recently, Vasko and Mitin examined the effect of SOI on frequency and angular distribution of the acoustic-phonon emission from a 2DEG, through calculating the differential energy flux of the phonon generation under the approximation of large polar angle scattering.[16] Unfortunately, most of the important natures for electron-phonon scattering in a spin-splitting 2DEG were not discussed in Ref. 16. In this paper, we will go beyond the approximation proposed by Ref. 16 and present a more exact solution to the problem. Moreover, this paper will present more detailed discussions about the unique features of electron-phonon interaction in a 2DEG in the presence of SOI. In Sec. II, the electronic transition rate induced by electron-phonon coupling in a 2DEG will be derived by including the SOI. The intensity of the acoustic-phonon generation can then be obtained by calculating electron-energy-loss-rate using a Boltzmann equation approach. These analytical results will be discussed in Sec. II. In Sec. III, the numerical results for the effect of SOI on acoustic-phonon emission will be presented and discussed for an InGaAs-based 2DEG. The results will also be compared with those reported in Ref. 16. The main conclusions of the present study will be summarized in Sec. IV.

II. ANALYTICAL RESULTS

In this paper, we consider a narrow-gap semiconductor quantum well in which SOI is induced by the Rashba effect. For a 2DEG in the *xy* plane, the single-electron Schrödinger equation including the lowest order of the SOI can be solved analytically.[9] In the absence of electron-phonon coupling, the electron wave function can be written as a row vector

$$\Psi_{\mathbf{k}n\sigma}(\mathbf{R}) = 2^{-1/2}[1, i\sigma(k_x + ik_y)/k]e^{i\mathbf{k}\cdot\mathbf{r}}\psi_n(z), \quad (1)$$

where $\mathbf{R}=(\mathbf{r},z)=(x,y,z)$, $\mathbf{k}=(k_x,k_y)$ is the electron wave vector along the 2D plane, $k=(k_x^2+k_y^2)^{1/2}$, n is an index for the nth electronic subband along the z direction, and $\sigma = \pm 1$ corresponds to the $\pm$ spin branches. The corresponding electron energy spectrum is

$$E_{n\sigma}(\mathbf{k}) = E_{n\sigma}(k) = \hbar^2 k^2/2m^* + \varepsilon_n + \sigma\alpha k, \quad (2)$$

where m^* is the electron effective mass and α is the Rashba parameter which measures the strength of the SOI. The electron wave function $\psi_n(z)$ and subband energy ε_n along the growth direction are determined by a spin-independent Schrödinger equation.

In the presence of electron-phonon coupling, the first-order steady-state electronic transition rate can be calculated using Fermi's golden rule. Using Eqs. (1) and (2) we have

$$W_{\sigma'\sigma}(n',\mathbf{k}';n,\mathbf{k}) = \frac{2\pi}{\hbar}\sum_{q_z}[N_Q + 1/2 \mp 1/2]|V_{\mathbf{Q}}|^2 h_{\sigma'\sigma}(\mathbf{k}',\mathbf{k}) \times G_{n'n}(q_z)\delta_{\mathbf{k}',\mathbf{k}+\mathbf{q}}\delta[E_{n'\sigma'}(\mathbf{k}') - E_{n\sigma}(\mathbf{k}) \mp \hbar\omega_Q], \quad (3)$$

which measures the possibility for scattering of an electron from a state $|\mathbf{k},n,\sigma>$ to a state $|\mathbf{k}',n',\sigma'>$ through emission (lower case) or absorption (upper case) of a phonon. Here, $\mathbf{Q}=(\mathbf{q},q_z)=(q_x,q_y,q_z)$ is the phonon wave vector, $V_{\mathbf{Q}}$ is the electron-phonon interaction coefficient, ω_Q is the phonon frequency, $N_Q=(e^{\hbar\omega_Q/k_BT}-1)^{-1}$ is the phonon occupation number, $G_{n'n}(q_z)=|<n'|e^{iq_z z}|n>|^2$ is the form factor of the electron-phonon scattering, and $h_{\sigma'\sigma}(\mathbf{k}',\mathbf{k}) = (1+\sigma'\sigma\mathbf{k}'\cdot\mathbf{k}/k'k)/2$ is a spin-dependent matrix element.

In this paper, we consider that acoustic-phonon emission is generated and detected in a phonon emission experiment[1,4] in which (i) a pulsed electric field is applied along the x direction; (ii) electrons in the system are heated by this in-plane electric field and, therefore, can interact more strongly with phonons; and (iii) generated phonon waves can propagate in the system and phonon signals are detected by using, e.g., superconducting tunnel junction phonon spectrometers[4] placed at a certain angle to the growth direction of the 2DEG. It has been shown both experimentally[5] and theoretically[17] that the power signals detected in the phonon emission experiment can be described by the electron-energy-loss-rate (EELR) induced by electron-phonon coupling. Thus, in conjunction with the phonon emission experiments, one needs to study the EELR due to the electron-phonon scattering.

When a dc electric field F_x is applied along the x direction of a 2DEG, the corresponding semiclassical Boltzmann equation, for a case of nondegenerate statistics, reads

$$-\frac{eF_x}{\hbar}\frac{\partial f_{n\sigma}(\mathbf{k})}{\partial k_x} = \sum_{\mathbf{k}',n',\sigma'}[f_{n'\sigma'}(\mathbf{k}')W_{\sigma\sigma'}(n,\mathbf{k};n',\mathbf{k}') - f_{n\sigma}(\mathbf{k})W_{\sigma'\sigma}(n',\mathbf{k}';n,\mathbf{k})], \quad (4)$$

where $f_{n\sigma}(\mathbf{k})$ is the momentum-distribution function for an electron in a state $|\mathbf{k},n,\sigma>$. Assuming that $f_{n\sigma}(\mathbf{k})$ can be described by a drifted energy-distribution function, at the first-moment, the energy-balance equation[18] can be derived by multiplying $E_{n\sigma}(\mathbf{k})$ to both sides of the Boltzmann equation and summing over $\mathbf{k}$, n and σ. For the case of a relatively weak electric field F_x, the EELR per electron becomes (see the Appendix)

$$P = \frac{m^*}{2\pi\hbar^3 n_e s}\sum_{\mathbf{Q}}[N_Q + 1/2 \mp 1/2]\hbar\omega_Q|V_{\mathbf{Q}}|^2 \times \sum_{n',n}G_{n'n}(q_z)\sum_{\sigma,\sigma}\int_0^\infty dk\, f(E_{n\sigma}(k)) \times \frac{\Theta(X_+)I(k,X_+) + \Theta(X_-)I(k,X_-)}{\sqrt{(k+\sigma k_\alpha)^2 + y_{n'n}}}, \quad (5)$$

where $s = 1 - (\alpha/4\pi n_e)\Sigma_{n,\sigma}\int_0^\infty dk\, k(\sigma k + k_\alpha)f'(E)|_{E=E_{n\sigma}(k)}$ is a normalization factor, $f'(x)=\partial f(x)/\partial x$, $k_\alpha = m^*\alpha/\hbar^2$, $\Theta(x)$ is a unit-step-function, $y_{n'n} = (2m^*/\hbar^2)(\varepsilon_n - \varepsilon_{n'} \pm \hbar\omega_Q)$, $X_\pm = -\sigma' k_\alpha \pm \sqrt{(k+\sigma k_\alpha)^2 + y_{n'n}}$, $I(k,x) = \mathrm{Re}\{[(x+k)^2 - q^2]/[q^2 - (x-k)^2]\}^{\sigma'\sigma/2}$, and n_e is the total electron density of the 2DEG. For case of a narrow-width quantum well in which only the lowest electronic subband is present (i.e., $n'=n=0$), Eq. (5) becomes

$$P = \sum_{\mathbf{Q}}P(\mathbf{Q})\sum_{\sigma',\sigma}\{(N_Q+1)[I^+_{\sigma'\sigma}(\mathbf{Q}) + I^-_{\sigma'\sigma}(\mathbf{Q})] - N_Q[J^+_{\sigma'\sigma}(\mathbf{Q}) + J^-_{\sigma'\sigma}(\mathbf{Q})]\}, \quad (6a)$$

where

$$P(\mathbf{Q}) = \frac{m^*}{2\pi\hbar^3 n_e s}\hbar\omega_Q|V_{\mathbf{Q}}|^2 G_0(q_z) \quad (6b)$$

and $G_0(q_z) = G_{00}(q_z)$. Furthermore,

$$I^\pm_{\sigma'\sigma}(\mathbf{Q}) = \int_0^\infty \frac{dk\, f(E_\sigma(k))}{\sqrt{(k+\sigma k_\alpha)^2 - k_Q^2}}\Theta[(k+\sigma k_\alpha)^2 - k_Q^2] \times \Theta(x_\pm)I(k,x_\pm) \quad (6c)$$

for phonon emission and

$$J^\pm_{\sigma'\sigma}(\mathbf{Q}) = \int_0^\infty \frac{dk\, f(E_\sigma(k))}{\sqrt{(k+\sigma k_\alpha)^2 + k_Q^2}}\Theta(y_\pm)I(k,y_\pm) \quad (6d)$$

for phonon absorption. Here, $E_\sigma(k) = E_{0\sigma}(k)$, $k_Q^2 = 2m^*\omega_Q/\hbar$, $x_\pm = -\sigma' k_\alpha \pm [(k+\sigma k_\alpha)^2 - k_Q^2]^{1/2}$, and $y_\pm = -\sigma' k_\alpha \pm [(k+\sigma k_\alpha)^2 + k_Q^2]^{1/2}$. The terms $I^\pm_{\sigma'\sigma}(\mathbf{Q})$ and $J^\pm_{\sigma'\sigma}(\mathbf{Q})$ express the contributions to the EELR for electronic transition from spin branches σ' to σ. The $\pm$ sign in these terms implies that the SOI leads to two possible channels for electronic transition between the σ' and σ spin branches with the changes of the wave vector $\mathbf{k}'-\mathbf{k}=\mathbf{q}$ and energy $E_{\sigma'}(k') - E_\sigma(k) = \mp\hbar\omega_Q$, due to the nonparabolic feature of the electron energy spectrum (see the Appendix). The

physical reason behind this is that in the "−" spin branch, two states with different wave vectors (or momentums) may have the same energy.

Equation (6) reflects the fact that the net energy transfer rate due to electron-phonon coupling is the difference between phonon emission and phonon absorption by electron in the system. When the SOI is present in a 2DEG, the emission and absorption of phonons can be achieved through intra- and inter-SO electronic transitions. Moreover, electron-phonon interaction via phonon emission or absorption scattering should obey the momentum and energy conservation law, which has been reflected by the Θ-functions shown in Eq. (6). Below, on the basis of Eq. (6) I discuss the essential requirements to achieve an electron-phonon scattering event via electronic transition in different spin channels.

(1) For $\sigma'=\sigma=1$, $I^{-}_{++}(\mathbf{Q})=J^{-}_{++}(\mathbf{Q})=0$. When intra-SO electronic transition is within the "+" branch, phonon emission can be generated when kinetic energy of an electron $E=\hbar^2k^2/2m^*\geqslant\hbar\omega_Q-\alpha(\sqrt{k_\alpha^2+k_Q^2}-k_\alpha)$. Less requirement for E is needed for phonon absorption scattering.

(2) For $\sigma'=1$ and $\sigma=-1$, $I^{-}_{+-}(\mathbf{Q})=J^{-}_{+-}(\mathbf{Q})=0$. For inter-SO electronic transition from the "−" branch to the "+" branch, phonon emission can only be generated when $E\geqslant\hbar\omega_Q+\alpha(\sqrt{k_\alpha^2+k_Q^2}+k_\alpha)$; and phonon absorption can only be achieved when $\alpha k_\alpha/2\geqslant\hbar\omega_Q$ and $E\geqslant\alpha(\sqrt{k_\alpha^2-k_Q^2}+k_\alpha)-\hbar\omega_Q$ or $E\leqslant\alpha(k_\alpha-\sqrt{k_\alpha^2-k_Q^2})-\hbar\omega_Q$. These requirements are mainly due to the fact that the "+" branch has a higher energy level than the "−" branch has. Hence, the electronic transition from the "−" branch to the "+" branch is more favorable to the phonon absorption scattering.

(3) When $\sigma'=-1$ and $\sigma=1$, $J^{-}_{-+}(\mathbf{Q})=0$. For inter-SO electronic transition from $\sigma=1$ to $\sigma'=-1$, two scattering channels open up for phonon emission; one for $E\geqslant\hbar\omega_Q-\alpha(k_Q-k_\alpha/2)$ and another for $\hbar\omega_Q-\alpha(k_Q-k_\alpha/2)\leqslant E\leqslant\hbar\omega_Q-\alpha(\sqrt{k_\alpha^2+k_Q^2}-k_\alpha)$. This is because when transition is from the "+" branch to the "−" branch, there are two possible states in the "−" branch where the energy difference between these states and the initial state in the "+" branch is $\hbar\omega_Q$ and the change of the electron wave vector after a scattering event is q. There are less requirements of E for phonon absorption scattering but no contribution from $J^{-}_{-+}(\mathbf{Q})$ term. Thus, the electronic transition from the "+" spin branch to the "−" branch is more favorable to the phonon emission scattering.

(4) For $\sigma'=\sigma=-1$, four scattering channels open up for phonon emission when (i) $E\geqslant\hbar\omega_Q+\alpha(k_Q+k_\alpha/2)$; (ii) $E\leqslant\hbar\omega_Q-\alpha(k_Q-k_\alpha/2)$; (iii) $\hbar\omega_Q+\alpha(k_Q+k_\alpha/2)\leqslant E\leqslant\hbar\omega_Q+\alpha(\sqrt{k_\alpha^2+k_Q^2}+k_\alpha)$; and (iv) $\alpha k_\alpha/2\geqslant\hbar\omega_Q$ and $E\leqslant\hbar\omega_Q-\alpha(k_Q-k_\alpha/2)$. There are two channels for phonon absorption scattering with less requirement for E. Again, this is because in the "−" branch, two states with different wave vectors may have the same energy.

The results discussed above indicate that in the presence of SOI, electron-phonon interaction in a 2DEG has some unique features. The presence of SOI in a 2DEG can open up new channels for electronic transition accompanied by emission or absorption of phonons. Phonon emission and absorption then can be achieved through intra- and inter-SO electronic transitions. However, the requirement of momentum and energy conservation for an electron-phonon scattering event results in some selection rules according to different scattering channels. Moreover, because electron-phonon coupling is essentially an inelastic scattering mechanism, emission or absorption of phonons via intra- and inter-SO electronic transitions can change the spin orientation of electrons and, consequently, alter the spin polarization of the device system.

From now on, I limit myself to the case of acoustic-phonon generation. To investigate the frequency and angular distribution of the acoustic-phonon emission, it is convenient to define the phonon wave vector in polar coordinates $\mathbf{Q}=Q(\sin\theta\cos\phi,\sin\theta\sin\phi,\cos\theta)$, where θ is the polar angle to the z axis (or the growth direction) and ϕ is the azimuthal angle to the x direction along which the driven electric field is applied. Thus, θ and ϕ also define the phonon emission angle in the phonon emission experiment. The total EELR per electron due to electron–acoustic-phonon scattering [given by Eq. (6)] can then be written as

$$P=\int_0^\infty d\omega_Q\int_0^{2\pi}d\phi\int_0^{\pi}d\theta\,P_0(\mathbf{Q})\sin\theta. \tag{7}$$

Here, $\omega_Q=v_sQ$ is the acoustic-phonon frequency with v_s being the sound velocity of the material and

$$P_0(\mathbf{Q})=\frac{Q^2P(\mathbf{Q})}{(2\pi)^3v_s}\sum_{\sigma',\sigma}\{(N_Q+1)[I^{+}_{\sigma'\sigma}(\mathbf{Q})+I^{-}_{\sigma'\sigma}(\mathbf{Q})] - N_Q[J^{+}_{\sigma'\sigma}(\mathbf{Q})+J^{-}_{\sigma'\sigma}(\mathbf{Q})]\} \tag{8}$$

is the frequency and angular distribution function for acoustic-phonon emission.

III. NUMERICAL RESULTS

Here we consider an InGaAs-based 2DEG system in which both surface and bulklike acoustic-phonon modes are present. In phonon emission experiment, only the bulklike acoustic phonons can propagate along the growth direction and reach the phonon detectors located at a fixed angle to the growth direction. Thus, in the calculations, only electron interactions with bulklike acoustic phonons are included. In InGaAs, which has a zinc-blende lattice structure, the electron–acoustic-phonon interaction is mainly through deformation potential and piezoelectric coupling. It is well known[5,6] that piezoelectric coupling leads to the emission of low-frequency acoustic phonons at relatively low-excitation levels or electron temperature $T_e<5$ K, whereas deformation-potential coupling generates high-frequency acoustic phonons at intermediate excitations where $5<T_e<30$ K. In the present study, we focus on phonon emission via deformation potential coupling at intermediate excitation levels. For InGaAs, only the longitudinal phonon mode is connected with the deformation potential and we therefore have

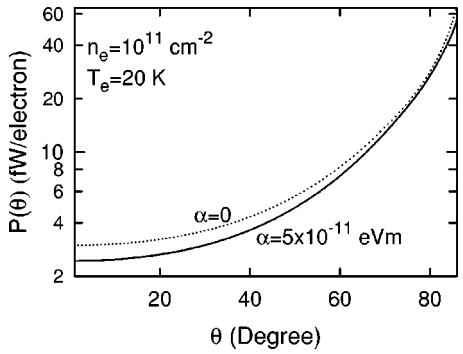

FIG. 1. Total power of phonon emission as a function of the polar angle θ to the growth direction for different Rashba parameters α. Here, $P(\theta)=\int_0^\infty d\omega_Q P_0(\mathbf{Q})$, $P_0(\mathbf{Q})$ is given by Eq. (8), $P(\theta)$ does not depend on ϕ angle, and $\alpha=0$ corresponds to a spin-degenerate 2DEG.

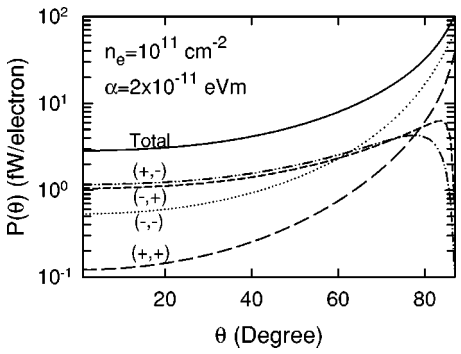

FIG. 2. Contribution from different scattering channels to total power of phonon emission as a function of θ angle at a fixed Rashba parameter as indicated. Here (σ,σ') corresponds to the transition from a spin branch σ to a branch σ'.

$$|V_{\mathbf{Q}}|^2=\frac{\hbar E_D^2\omega_Q}{2\rho v_s^2}. \tag{9}$$

Here E_D, ρ, and v_s are, respectively, the deformation potential constant, density, and longitudinal sound velocity of the material. This paper assumes that the applied electric field is low enough so that the hot-phonon effects are negligible. We take the lattice temperature $T=2$ K at which an aluminum bolometer can be used as phonon signal detector.[5] Furthermore, the Fermi–Dirac function is taken as the electron distribution function where the electron temperature is taken as $T_e=20$ K.

For an InGaAs/InAlAs heterojunction, the usual triangular well approximation can be applied to model the confining potential normal to the interface. Thus, $G_0(q_z)$ can be calculated analytically. The material parameters for InGaAs are known:[19] (i) the electron effective mass $m^*=0.042m_e$ with m_e being the electron rest mass; (ii) the density of material $\rho=5.66$ g/cm^3; (iii) the longitudinal sound velocity $v_s=4.3\times10^5$ cm/s; (iv) the deformation potential constant $E_D=11.7$ eV; and (v) the dielectric constant $\kappa=14.6$. Moreover, in the numerical calculations we use typical sample parameters for an InGaAs-based 2DEG. The total density of the 2DEG is taken as $n_e=10^{11}$ cm^{-2} and the depletion charge density $N_{\text{depl}}=5\times10^{10}$ cm^{-2}. Very recent experimental results[13] have indicated that in these spintronic systems, the Rashba parameter can reach up to $\alpha\sim3$–4×10^{-11} eV m.

The total power of acoustic-phonon emission, $P(\theta)=\int_0^\infty d\omega_Q P_0(\mathbf{Q})$ detected at an angle (θ,ϕ), is shown in Fig. 1 as a function of the θ angle for different Rashba parameters α. Here $P_0(\mathbf{Q})$ is given by Eq. (8) and $\alpha=0$ is the case without including SOI in a 2DEG. It should be noted that for phonon emission via deformation potential coupling, $P_0(\mathbf{Q})$ depends only on $q=(q_x^2+q_y^2)^{1/2}$ and q_z. As a result, phonon emission does not depend on the ϕ angle even when SOI is present. The angular and frequency dependence of the acoustic-phonon emission is mainly induced by (i) the requirement of momentum and energy conservation during a scattering event; (ii) the electron-phonon coupling coefficient; and (iii) the form factor for electron-phonon interaction. From Fig. 1, we see that the intensity of phonon emission increases with increasing polar angle θ, which implies that strong phonon signals can be detected at large θ angles close to $\theta=90°$. It is interesting to note that the presence of SOI does not change significantly the angular dependence of the phonon generation and, unexpectedly, the intensity of the phonon emission is actually reduced slightly by the SOI. The physical reason behind this is that although the presence of SOI in a 2DEG can open up new channels for electronic transition accompanied by the emission of phonons, the selection rules induced by the requirement of momentum and energy conservation during a scattering event (as discussed previously) can reduce the overall possibility for electron-phonon coupling in different spin branches. An important conclusion obtained here is that in the presence of SOI, the intensity of acoustic-phonon generation via deformation potential coupling in a 2DEG does not differ significantly from that obtained in the absence of SOI.

The contribution from different scattering channels to intensity of phonon generation $P(\theta)$ is plotted in Fig. 2 as a function of θ angle at a fixed Rashba parameter. For a spin-split 2DEG, electronic transition accompanied by the emission of phonons can be achieved through intra- and inter-SO scattering channels. The results shown in Fig. 2 indicate that in the small θ angle regime ($\theta<60°$ for $\alpha=2\times10^{-11}$ eV m), acoustic-phonon emission is mainly generated via inter-SO electronic transitions. At large θ angles ($\theta>60°$), phonon signals come mainly from intra-SO scattering. This is mainly due to the fact that inter-SO transition requires a smaller momentum change than intra-SO transition does. Because electronic transition from spin branch $\sigma=1$ to the branch $\sigma'=-1$ [i.e. $(+,-)$ channel] corresponds to the scattering of an electron from a higher energy state to a lower one, phonon emission is more possibly generated via $(+,-)$ channel than via $(-,+)$ one. Furthermore, in the presence of SOI, more electrons are in the "$-$" spin branch because it has a lower energy and more density of states.[20] As a result, intra-SO electronic transitions accompanied by the emission of phonons can be more possibly achieved in the "$-$" spin branch. It should be noted that a large polar angle θ to the z axis corresponds to a small angle scattering of a 2DEG in the xy plane. It has been demonstrated

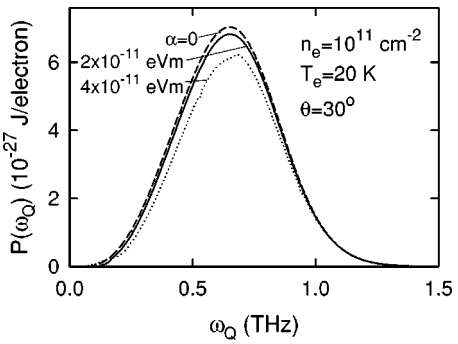

FIG. 3. Frequency distribution of the acoustic-phonon emission detected at $\theta=30°$ for different Rashba parameters. Here $P(\omega_Q)=P_0(\mathbf{Q})$ given by Eq. (8) does not depend on the ϕ angle.

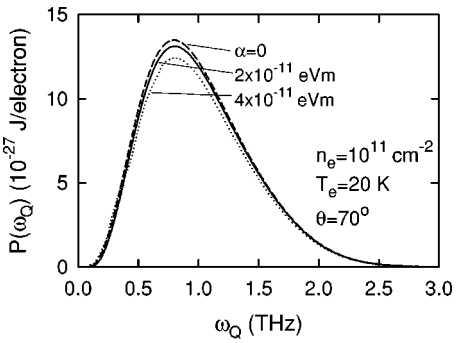

FIG. 5. Frequency distribution of the phonon generation at an angle $\theta=70°$ for different Rashba parameters. Here $P(\omega_Q)=P_0(\mathbf{Q})$ given by Eq. (8).

experimentally[15] that the events of small angle scattering in the 2D plane of a 2DEG do not change spin orientation of electrons significantly. Consequently, physical quantities determined by small angle electronic scattering, such as quantum lifetimes in different spin orbits, depend weakly on SOI.[15] One important conclusion drawn from Fig. 2 is that at large phonon emission angle $\theta\sim 90°$, acoustic-phonon scattering does not alter significantly the spin orientation of the 2DEG, where phonon emission is mainly generated via intra-SO transitions. At a small θ angle, acoustic-phonon scattering is mainly achieved via inter-SO transition during which spin orientation of an electron has to be exchanged.

The frequency distribution of the acoustic-phonon emission detected at a relatively small polar angle $\theta=30°$ is shown in Fig. 3 for different Rashba parameters. With increasing α, SOI increases and intensity of phonon emission decreases slightly similar to those shown in Fig. 1. The results shown in Fig. 3 implies that the presence of SOI does not change significantly the frequency distribution of acoustic-phonon emission via deformation potential coupling, where generated phonon frequency is at about $f=\omega_Q/2\pi\sim 0.1$ THz. The contribution from different scattering channels to frequency distribution of the phonon emission at $\theta=30°$ is shown in Fig. 4 at a fixed α. In low-frequency regime ($\omega_Q<0.3$ THz at $\alpha=2\times10^{-11}$ eV m), intra-SO transition within the "$-$" branch contributes a major source of the phonon signal, and inter-SO scattering $(-,+)$ results mainly in phonon absorption which gives a negative contribution to the intensity of phonon generation. When $\omega_Q>0.3$ THz, phonon emission is dominated by inter-SO scattering and contribution from the $(+,-)$ channel is larger than that from the $(-,+)$ one.

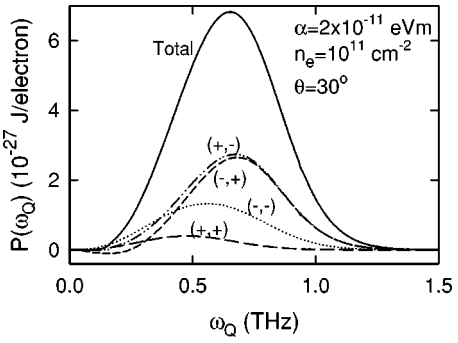

FIG. 4. Contribution from different scattering channels to intensity of phonon generation versus phonon frequency at a fixed θ angle and a fixed α. Here $P(\omega_Q)=P_0(\mathbf{Q})$ given by Eq. (8) and (σ,σ') corresponds to the transition from a spin branch σ to a branch σ'.

In Fig. 5 the spectrum of the acoustic-phonon emission is shown at a relatively large polar angle $\theta=70°$ for different Rashba parameters. Again, the SOI in a 2DEG affects weakly the frequency distribution of the phonon emission detected at $\theta=70°$. Compared with phonon signals detected at $\theta=30°$ (see Fig. 3), one finds that at $\theta=70°$ a much more broadened phonon spectrum can be observed. This implies that higher-frequency acoustic-phonon emission can be detected at a larger θ angle. The contribution to the line shape of the phonon spectrum from different scattering channels is plotted in Fig. 6 for $\theta=70°$ and $\alpha=2\times10^{-11}$ eV m. When $\omega_Q<1$ THz, phonon emission is mainly achieved via intra-SO transition within the "$-$" spin branch. The emission of high-frequency phonons ($\omega_Q>1.2$ THz) is mainly due to inter-SO scattering in the channels $(-,+)$ and $(+,-)$. The results shown in Figs. 4 and 6 indicate that in the presence of SOI, electrons interact more strongly with low-frequency acoustic phonons via intra-SO scattering channels. In such a case, low-frequency acoustic-phonon scattering does not change significantly the spin orientation of the electrons. On the other hand, when inter-SO scattering channels open up, electrons can interact more strongly with

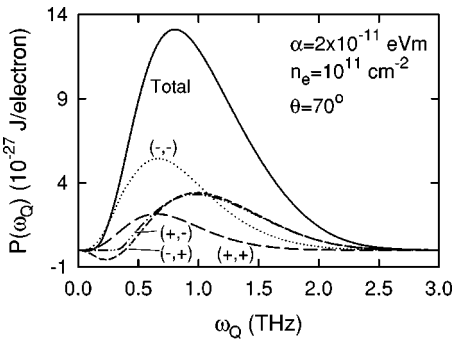

FIG. 6. Contribution to generated phonon frequency from different scattering channels detected at $\theta=70°$ at a fixed α parameter.

high-frequency acoustic phonons via exchanging of their spin orientations. These theoretical results suggest that the spin polarization of a 2DEG can only be altered significantly when electrons are scattered by high-frequency acoustic phonons.

The theoretical results shown above indicate that the frequency and angular distribution of the acoustic-phonon emission from a splitting-split 2DEG does not differ significantly from those observed in the phonon emission experiments for spin-degenerate 2DEGs. However, it is found that if the phonon detector is placed at a small polar angle $\theta \sim 0°$ to the growth direction, phonon signals are mainly generated via inter-SO electronic transitions. When the phonon detector is placed at a large angle $\theta \sim 90°$, intra-SO transitions contribute a major source of the phonon signal. On the basis that phonon emission experiments[1,4] can measure the angular distribution of the phonon generation, these experimental techniques can then be used to examine spin-dependent electronic transitions in spintronic systems. Moreover, since the strength of the SOI in InGaAs-based spintronic devices can be controlled by applying a gate voltage[14] or varying the sample growth parameters,[15] it is therefore expected that these predictions can be tested in the near future.

From a theoretical point of view, there is no essential difference of the frequency and angular distribution function for phonon emission obtained from using an energy-balance equation approach developed here or from using directly the differential energy flux proposed in Ref. 16. However, in order to carry out an angle integration, Ref. 16 assumed $\sin\theta \gg v_s/v_F$, where θ is an angle between $\mathbf{k}$ and $\mathbf{k}'$ and v_F is the Fermi velocity. Noting that θ used in Ref. 16 is basically the same as θ defined in this paper, the approximation applied by Ref. 16 corresponds therefore to the case of large θ angle scattering discussed in the present paper. It should be noted that the angle integration mentioned in Ref. 16 has been carried out exactly and analytically in the present study (see the Appendix). Hence, this paper presents a more exact solution to the problem. As discussed previously in this section, a large θ angle corresponds to a small angle scattering of a 2DEG in the *xy* plane. With increasing θ, the inter-SO scattering rate can be reduced and intra-SO scattering can become dominant (see Fig. 2). Thus, the approximation used in Ref. 16 may result in an under-evaluation of the contribution from inter-SO transitions in relatively small θ angle regime and from high-frequency acoustic-phonon scattering. It has been shown in this section that inter-SO transition leads to the emission of high-frequency acoustic phonons and dominates phonon generation in the small θ angle regime. After comparing the results obtained from this study with those reported in Ref. 16, one finds that (i) the inclusion of the high-frequency acoustic-phonon emission via inter-SO transitions can smooth the high-frequency cutoff of the phonon spectrum reported in Ref. 16 (see Figs. 3 and 5 in this paper and Fig. 2 in Ref. 16); (ii) at a small θ angle, phonon emission is mainly generated via inter-SO transitions (see Fig. 4) and, therefore, the more broadened spectrum at a smaller θ angle shown in Fig. 2 in Ref. 16 is a consequence of the under-evaluation of inter-SO generation; and (iii) because the contribution from high-frequency phonon emission via inter-SO transitions in the small θ angles has been included here, the significant blueshift of the phonon spectrum with decreasing θ shown in Fig. 2 in Ref. 16 cannot be reproduced in the present paper. Furthermore, the contributions from different scattering channels to the generation of acoustic-phonon emission has been examined in this paper. This can be more helpful to understand the unique feature of electron-phonon interaction in a 2DEG in the presence of SOI.

IV. SUMMARY

In this paper, I have examined the effects of SOI, induced by the Rashba effect, on emission and scattering of phonons in general and acoustic phonons in particular in 2DEG systems. It has been found that SOI in a 2DEG can result in some unique features for electron-phonon interaction. In conjunction with a phonon emission experiment, I have developed a simple theory to study the frequency and angular dependence of the acoustic-phonon generation from a spin split 2DEG. The influence of the SOI on acoustic-phonon emission has been investigated for an InGaAs-based 2DEG. The main conclusions obtained from this study are summarized as follows.

(1) In the presence of SOI, new channels open up for electronic transition around the Fermi level accompanied by the emission and absorption of phonons. As a result, phonon scattering and generation can be achieved via intra- and inter-SO electronic transitions. However, the requirement of momentum and energy conservation during an electron-phonon scattering event introduces some selection rules for electron-phonon coupling in different scattering channels. These selection rules may reduce slightly the overall strength of the electron-phonon interaction.

(2) The presence of SOI does not change significantly the spectrum and emission angle of the acoustic-phonon generation via deformation potential coupling, compared to the case without inclusion of SOI in a 2DEG. For a typical InGaAs-based 2DEG, the frequency of the acoustic-phonon emission can be generated at about $f \sim 0.1$ THz and strong phonon signals can be detected at a large polar angle to the growth direction.

(3) At a large polar angle $\theta \sim 90°$, which corresponds to a small angle scattering of a 2DEG in the 2D plane, electron-phonon scattering is mainly achieved via intra-SO transitions. In such a case, spin orientation of an electron does not alter significantly by acoustic-phonon scattering. This is in line with experimental results obtained from magnetotransport measurements,[15] where very little difference of the quantum lifetimes in different spin branches has been observed. At small θ angles, the electron-phonon scattering is mainly through inter-SO transition channels. As a result, the exchange of spin orientation of electrons can be achieved via acoustic-phonon scattering at small polar angles. Furthermore, low-frequency acoustic-phonon emission is generated mainly via intra-SO scattering, whereas high-frequency acoustic-phonon signals come mainly from inter-SO transitions.

These theoretical results suggest that in a spintronic sys-

tem, spin polarization of electrons can only be changed significantly when channels for high-frequency acoustic-phonon scattering open up at relatively small polar angles to the growth direction. The author hopes that the results presented and discussed in this paper will be helpful in designing the spintronic materials and in applying the spintronic systems as high-frequency hypersonic devices.

ACKNOWLEDGMENTS

The author acknowledges financial support from the Australian Research Council via an ARF Research Fellowship Program. Discussions with P. Vasilopoulos (Concordia University, Canada) are gratefully acknowledged.

APPENDIX

To obtain Eq. (5), one needs to calculate

$$II(k,q)=\int_0^{2\pi} d\theta\, g(\theta)\,\delta(\hbar^2X^2/2m^*+\sigma'\alpha X-\hbar^2k^2/2m^* - \sigma\alpha k-\hbar^2 y_{n'n}/2m^*), \tag{A1}$$

where θ is an angle between $\mathbf{k}$ and $\mathbf{q}$, $y_{n'n}=2m^*(\varepsilon_n-\varepsilon_{n'} \pm\hbar\omega_Q)/\hbar^2$, and $X=k'=|\mathbf{k}+\mathbf{q}|=\sqrt{k^2+q^2+2kq\cos\theta}$ determined by the momentum conservation law. Noting that (i) the δ-function in Eq. (A1) represents the energy conservation law during an electron-phonon scattering event; (ii) there are possibly two real and positive roots for X determined from a nonparabolic function $\hbar^2X^2/2m^*+\sigma'\alpha X=\varepsilon$; and (iii) X is the absolute value of the electron wave vector in the final state after scattering and, therefore, X should be real and positive, we have $II(k,q)=II_+(k,q)+II_-(k,q)$, where

$$II_\pm(k,q) = \frac{m^*}{\hbar^2}\frac{\Theta(X_\pm)\Theta[4k^2q^2-(X_\pm^2-k^2-q^2)^2]g(\theta_\pm)X_\pm}{\sqrt{(k+\sigma k_\alpha)^2+y_{n'n}}\sqrt{4k^2q^2-(X_\pm^2-k^2-q^2)}}. \tag{A2}$$

Here $\Theta(x)$ is a unit step function, $X_\pm=-\sigma' k_\alpha \pm\sqrt{(k+\sigma k_\alpha)^2+y_{n'n}}$, and $\theta_\pm$ is determined by solving $X_\pm=\sqrt{k^2+q^2+2kq\cos\theta_\pm}$. It should be noted that in the presence of SOI, two roots $X_\pm$ implies two possible channels for electronic transitions which satisfy the momentum and energy conservation laws, when initial state of an electron is at $|\mathbf{k},n,\sigma>$. This is in sharp contrast to the case of a spin-degenerate 2DEG (i.e., $\alpha=0$) where a parabolic energy spectrum results in only one real and positive root for X from $\hbar^2X^2/2m^*=\varepsilon$.

*Email address: wen105@rsphysse.anu.edu.au

[1] L.J. Challis, A.J. Kent, and V.W. Rampton, Semicond. Sci. Technol. **5**, 1179 (1990); L.J. Challis, in *Low-Dimensional Semiconductor Structures*, edited by P.N. Butcher *et al.* (Plenum, New York, 1992).

[2] See, e.g., R.M. White, in *Topics in Solid State and Quantum Electronics*, edited by W.D. Hershberger (Wiley, New York, 1972).

[3] R.A. Höpfel and G. Weimann, Appl. Phys. Lett. **46**, 291 (1985); C.H. Yang, J.M. Carlson-Swindle, S.A. Lyon, and J.M. Worlock, Phys. Rev. Lett. **55**, 2359 (1985).

[4] V. Narayanamurti, Science **213**, 717 (1981); J.C. Hensel, R.C. Dynes, and D.C. Tsui, Phys. Rev. B **28**, 1124 (1983); M. Rothenfusser, L. Köster, and W. Dietsche, *ibid.* **34**, 5518 (1986).

[5] P. Hawker, A.J. Kent, L.J. Challis, M. Henini, and O.H. Hughes, J. Phys.: Condens. Matter **1**, 1153 (1989); P. Hawker, A.J. Kent, N. Hauser, and C. Jagadish, Semicond. Sci. Technol. **10**, 601 (1995); P. Hawker, A.J. Kent, O.H. Hughes, and L.J. Challis, *ibid.* **7**, B29 (1992).

[6] W. Xu, Phys. Rev. B **54**, 2775 (1996); W. Xu and C. Zhang, Europhys. Lett. **42**, 191 (1998).

[7] S. Das Sarma, J.K. Jain, and R. Jalabert, Phys. Rev. B **41**, 3561 (1990); X.L. Lei and M.W. Wu, *ibid.* **47**, 13338 (1990); J.R. Senna and S. Das Sarma, Phys. Rev. Lett. **70**, 2593 (1993); D.Y. Xing and C.S. Ting, *ibid.* **72**, 2812 (1994).

[8] S. Datta and B. Das, Appl. Phys. Lett. **56**, 665 (1990).

[9] X.F. Wang, P. Vasilopoulos, and F.M. Peeters, Phys. Rev. B **65**, 165217 (2002).

[10] G.A. Prinz, Phys. Today **48** (4), 58 (1995); C.H.W. Barnes, J.M. Shilton, and A.M. Robinson, Phys. Rev. B **62**, 8410 (2000).

[11] Th. Schäpers, G. Emgels, J. Lange, Th. Klocke, M. Hollfelder, and H. Lüth, J. Appl. Phys. **83**, 4324 (1998).

[12] E.I. Rashba, Sov. Phys. Solid State **2**, 1109 (1960); E. I. Rashba and V. I. Sheka, in *Landau Level Spectroscopy*, edited by G. Landwehr and E.I. Rashba (North-Holland, Amsterdam, 1991), Vol. 1, p. 131.

[13] Y. Sato, T. Kita, S. Gozu, and S. Yamada, J. Appl. Phys. **89**, 8017 (2001); D. Grundler, Phys. Rev. Lett. **84**, 6074 (2000).

[14] J. Nitta, T. Akazaki, H. Takayanagi, and T. Enoki, Phys. Rev. Lett. **78**, 1335 (1997).

[15] J. Luo, H. Munekata, F.F. Fang, and P.J. Stiles, Phys. Rev. B **41**, 7685 (1990).

[16] F.T. Vasko and V.V. Mitin, Phys. Rev. B **61**, 11047 (2000).

[17] W. Xu, Phys. Rev. B **51**, 13294 (1995).

[18] W. Xu, I. Khmyrova, and V. Ryzhii, Phys. Rev. B **64**, 085209 (2001).

[19] See, e.g., S. Adachi, *Physical Properties of III–V Semiconductor Compounds* (Wiley, New York, 1992).

[20] W. Xu, Appl. Phys. Lett. **82**, 724 (2003).